YMTHE, Volume *26*

Supplemental Information

Inhibition of Glycogen Synthase II with RNAi Prevents Liver Injury in Mouse Models of Glycogen Storage Diseases

Natalie Pursell, Jessica Gierut, Wei Zhou, Michael Dills, Rohan Diwanji, Monika Gjorgjieva, Utsav Saxena, Jr-Shiuan Yang, Anee Shah, Nandini Venkat, Rachel Storr, Boyoung Kim, Weimin Wang, Marc Abrams, Margaux Raffin, Gilles Mithieux, Fabienne Rajas, Henryk Dudek, Bob D. Brown, and Chengjung Lai

Supplementary Fig. S1. Glycogenesis and Glycogenolysis Pathways.

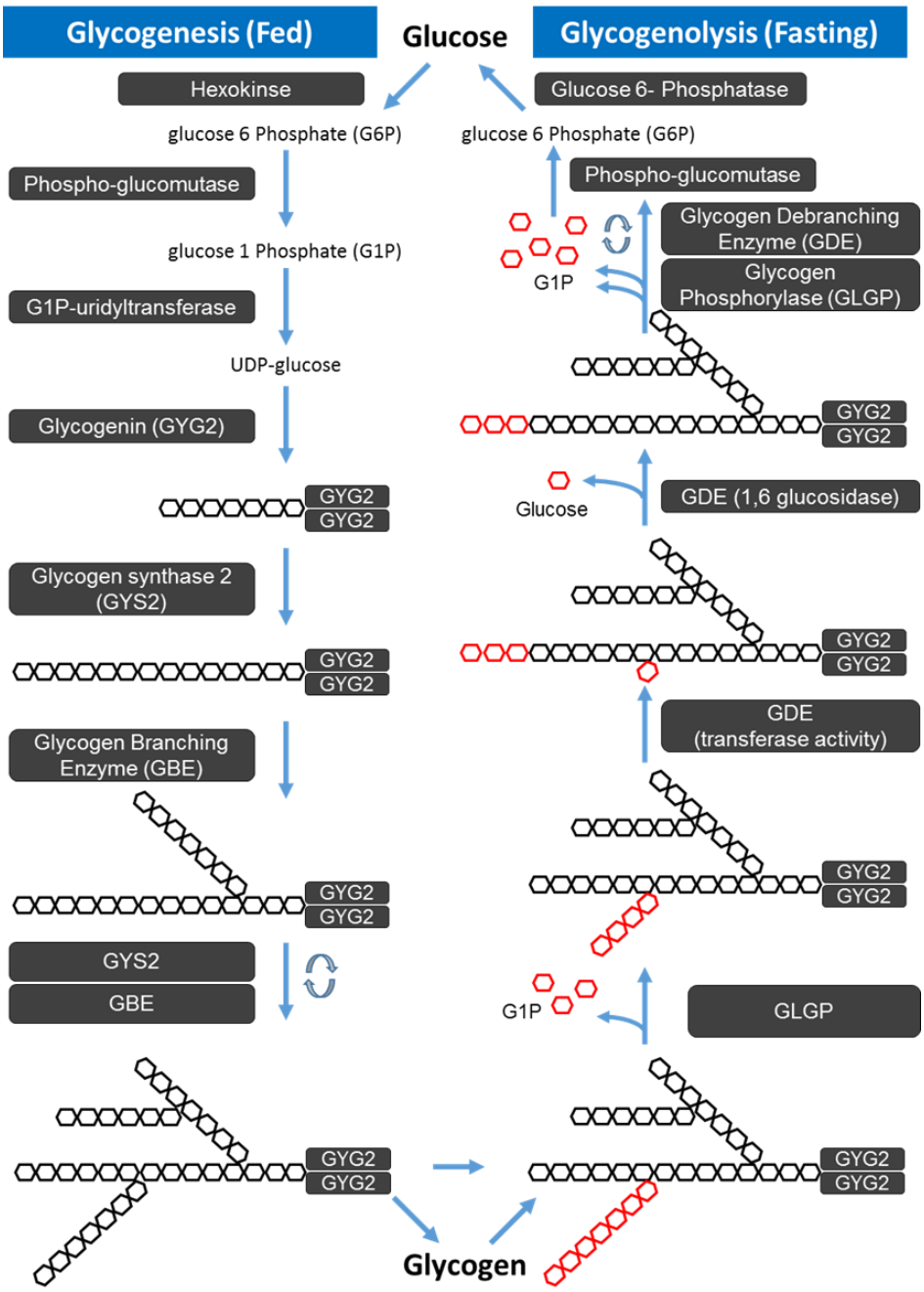

Supplementary Fig. S2. Identification of lead *Gys2* siRNAs.

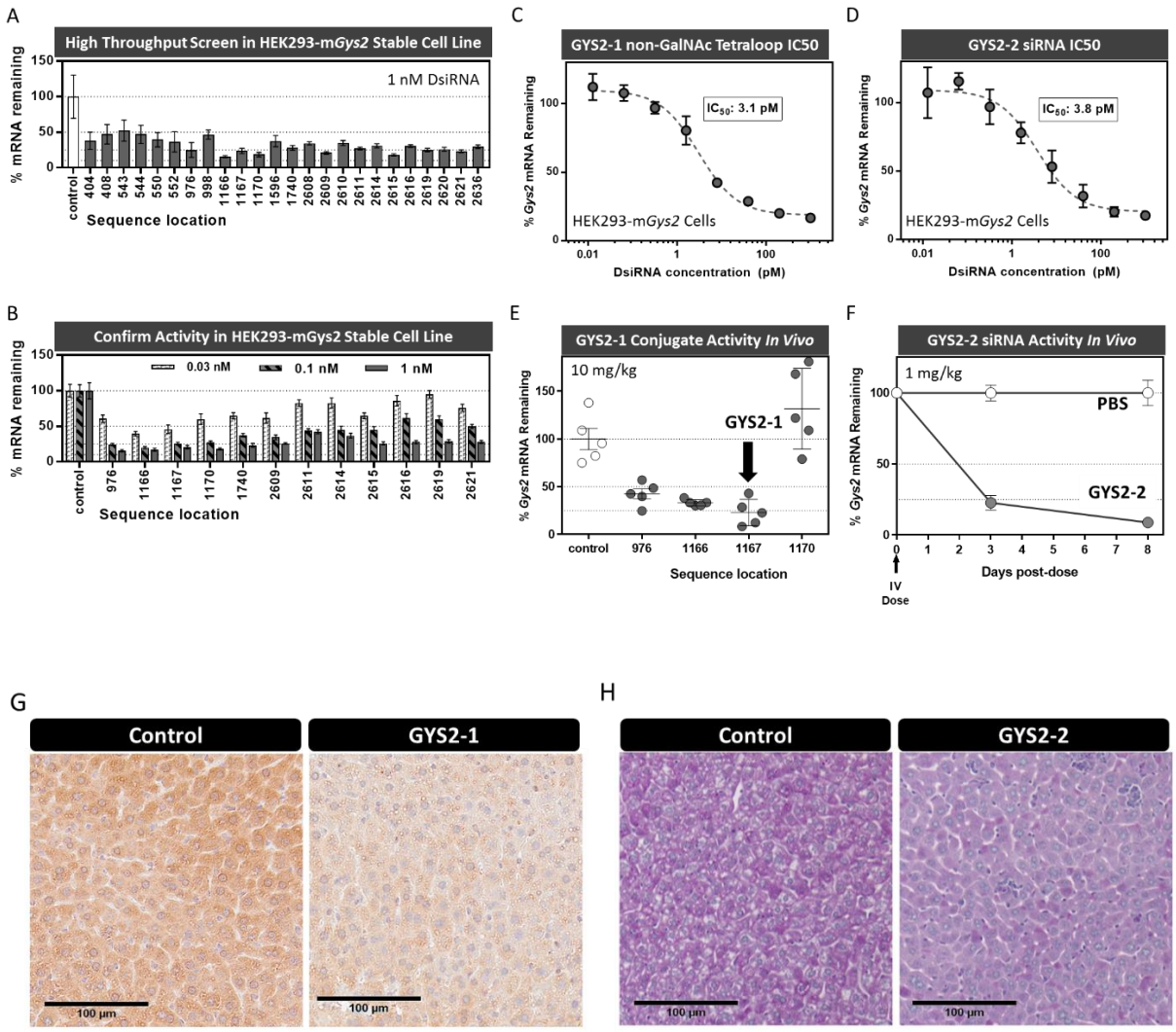

(A) Results from high-throughput screen of *Gys2* siRNA sequences in HEK293 cells stably expressing mouse *Gys2* mRNA (HEK293-mGys2) identifies potent sequences. (B) Activity of best siRNA sequences was confirmed in HEK293-mGys2 with a three-point dose-response. (C) *Gys2*-1167 sequences was converted into a tetraloop conjugate (no GalNAc sugar residues) and its IC50 determined in HEK293-mGys2 cells. (D) *Gys2*-1166 was selected as GYS2-2 and its IC50 measured in HEK293-mGys2 cells. (E) GalNAc sugar residues were added to GYS2-1 and other *Gys2* siRNA sequences for confirmation of potency *in vivo*. Wild-type mice were given a single, subcutaneous 10 mg/kg dose and sacrificed three days later. RNA was prepared from terminal liver samples and *Gys2* mRNA inhibition measured by RT-PCR. GYS2-1 shows approximately 75% reduction in *Gys2* mRNA. (F) GYS2-2 siRNA was formulated in lipid nanoparticle and intravenously injected into mice at 1 mg/kg. Mice were sacrificed three or eight days post-dose for RNA preparation and *Gys2* mRNA measurement by RT-PCR. (G) The results of immunohistochemistry indicate GYS2-1 reduces GYS protein expression in nearly all hepatocytes. (H) The results of PAS staining indicate GYS2-2 reduces glycogen accumulation in nearly all hepatocytes. Scale bar represents 100 µm.

Supplementary Fig. S3. *Gys2* mRNA Knockdown Prevents Abnormal Glycogen Accumulation and Hepatic Abnormalities in the *Agl*$^{-/-}$ GSD III mouse model.

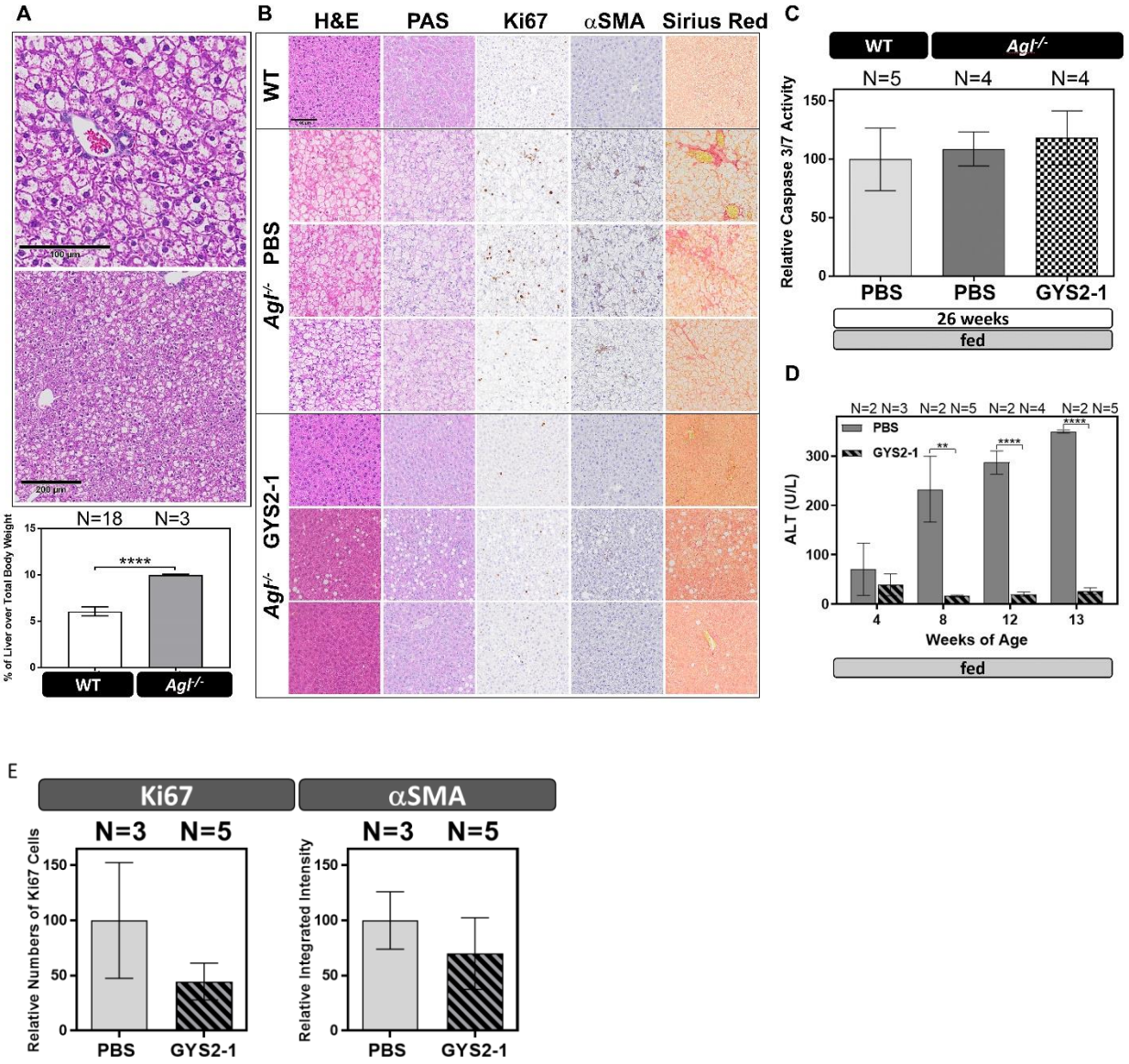

(A) *Agl*$^{-/-}$ mice develop hepatomegaly with abnormal histomorphology by four weeks of age. The liver-to-body weight ratio in *Agl*$^{-/-}$ mice is significantly increased compared to wildtype mice ($p<0.0001$). Scale bar represents 100 µm (upper panel) and 200 µm (lower panel). (B) *Agl*$^{-/-}$ mice treated with PBS or GYS2-1 for 10 doses starting at 4 weeks of age. Histological analysis indicates that GYS2-1 is able to prevent the development of abnormal histopathology of *Agl*$^{-/-}$ mice. In GYS2-1 treated animals, H&E or PAS stained liver sections showed a reduction of vacuoles formed from over-accumulation of glycogen molecules. Increased Ki67 positive cells were observed in *Agl*$^{-/-}$ mice and were reduced with GYS2-1 treatment. Sirius red staining and IHC for αSMA also indicate that GYS2-1 effectively reduces fibrosis of *Agl*$^{-/-}$ mice. Representative images of three individual animals from PBS or GYS2-2 treated groups are shown. Scale bar represents 100 µm. (C) Measurement of Caspase-3/7 activity in mouse liver extracts does not show an elevation of the activity of apoptotic Caspases 3 and 7. (D) *Agl*$^{-/-}$ mice show increasing signs of liver damage with

increasing age measured by quantification of blood ALT levels which is prevented by GYS2-1 treatment (** $p \leq 0.01$, **** $p < 0.0001$). (E) Quantitative analysis of IHC of Ki67 and α-SMA staining shown in (B).

Supplementary Fig. S4. Quantitative analysis of Ki67 staining in PBS or GYS2-1 treated GSD III, *Agl*$^{-/-}$ mice.

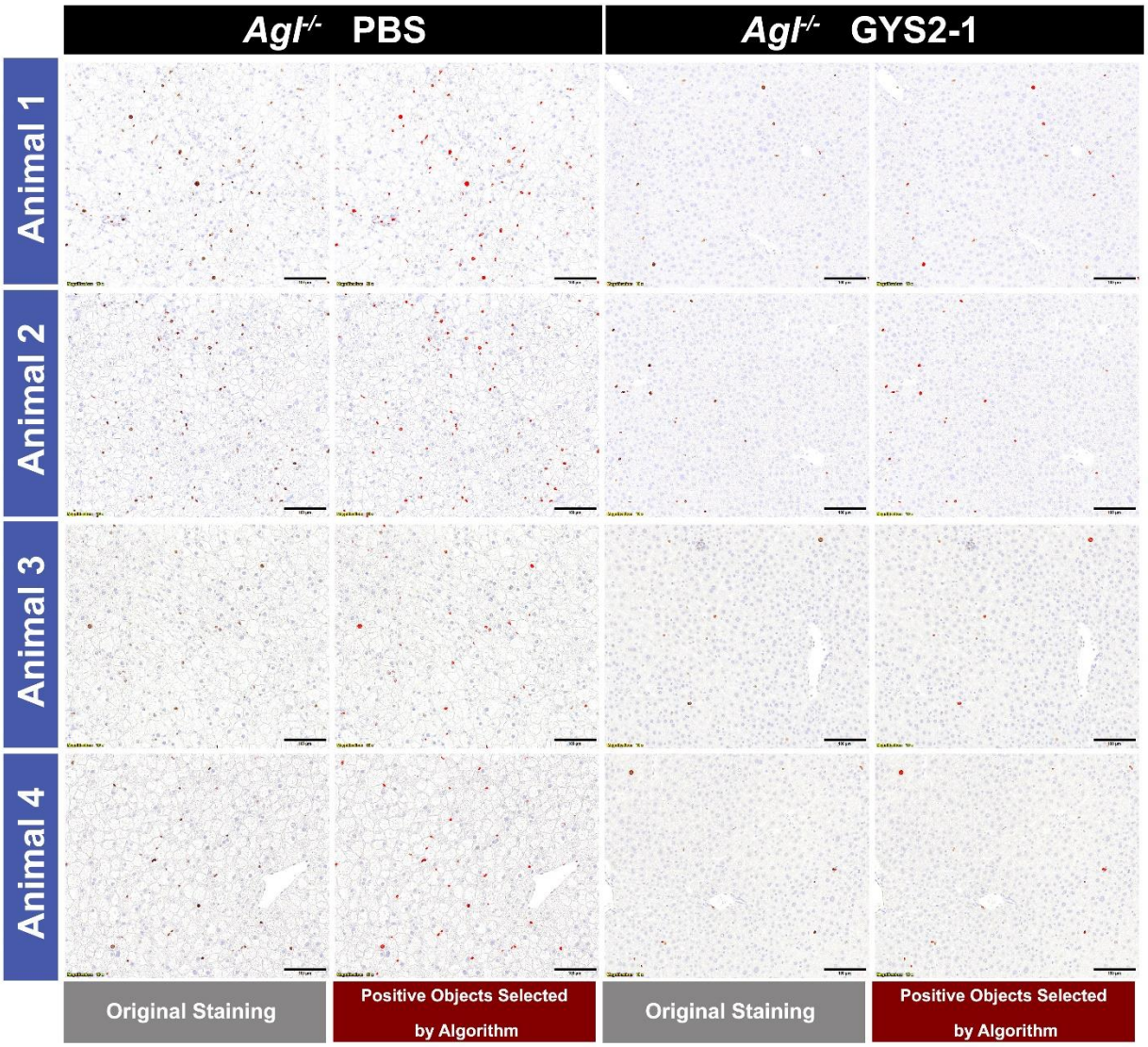

Quantitative analysis of K67 staining in the liver of *Agl*$^{-/-}$ mice treated with PBS or GYS2-1 weekly for 18 doses starting at 8 weeks of age was performed using Olympus cellSens software. Briefly, five ROIs (approximately 320,000 μm² each) of one representative liver section for each individual animal were scored and quantified using an algorithm with a pre-defined intensity threshold. Examples of positive object selection using the algorithm are shown. The total number of positive counts normalized to the total area quantified was compared for PBS or GYS2-1 treated animals and the results summarized in Fig. 3C. Scale bar represents 100 μm.

Supplementary Fig. S5. Quantitative analysis of αSMA staining in PBS or GYS2-1 treated GSD III, *Agl*$^{-/-}$ mice.

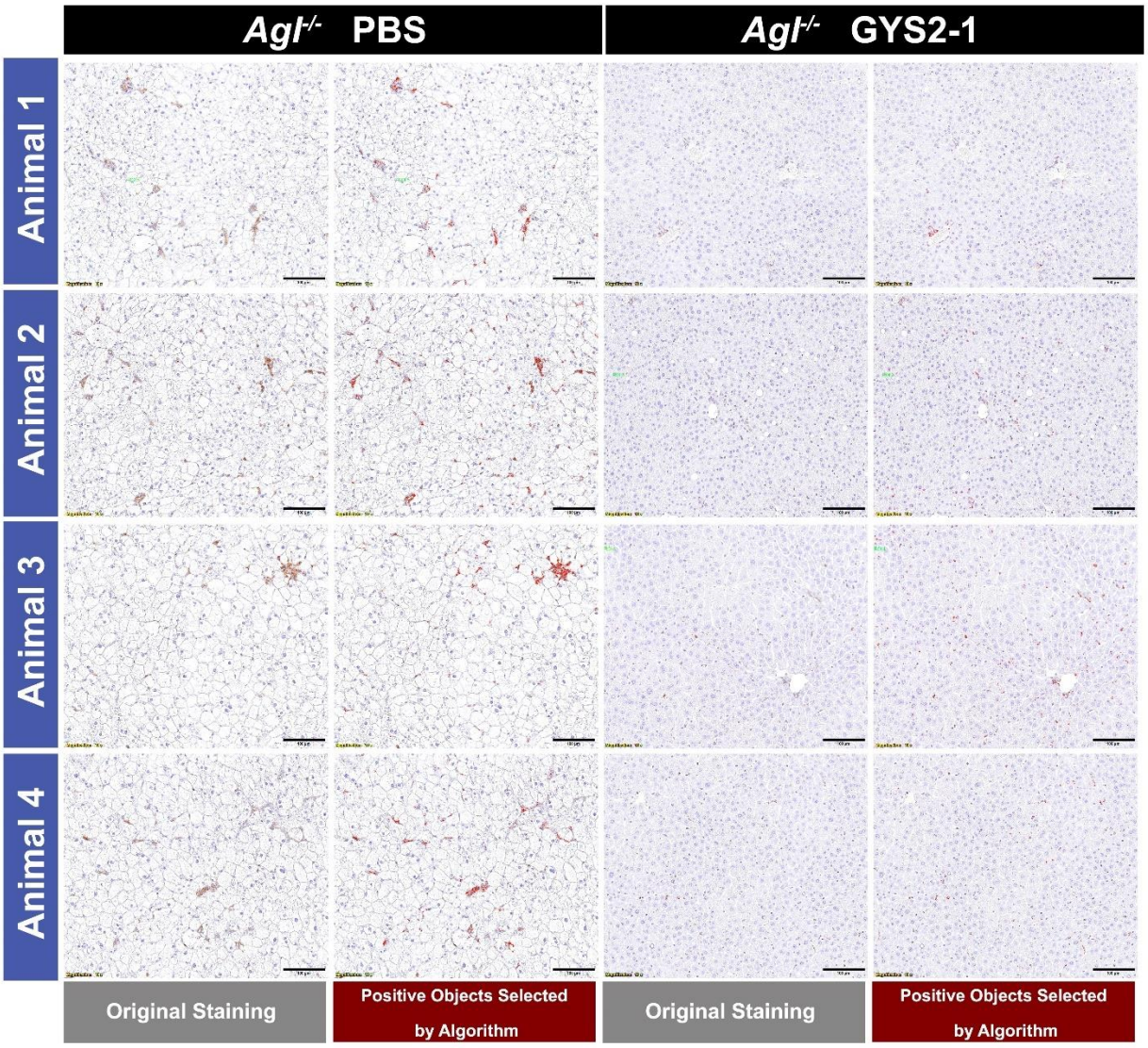

Quantitative analysis of αSMA staining in the liver of *Agl*$^{-/-}$ mice treated with PBS or GYS2-1 weekly for 18 doses starting at 8 weeks of age was performed using Olympus cellSens software. Briefly, five ROIs (approximately 320,000 μm² each) of one representative liver section for each individual animal were scored and quantified using an algorithm with a pre-defined intensity threshold. Certain areas were intentionally excluded from quantification in order to minimize the signal contributing from smooth muscles of large blood vessels. Examples of positive object selection using the algorithm are shown. The sum intensity normalized to the total area quantified was compared for PBS or GYS2-1 treated animals and the results summarized in Fig. 3C. Scale bar represents 100 μm.

Supplementary Fig. S6. Quantitative analysis of Sirius Red staining in PBS or GYS2-1 treated GSD III, *Agl*$^{-/-}$ mice.

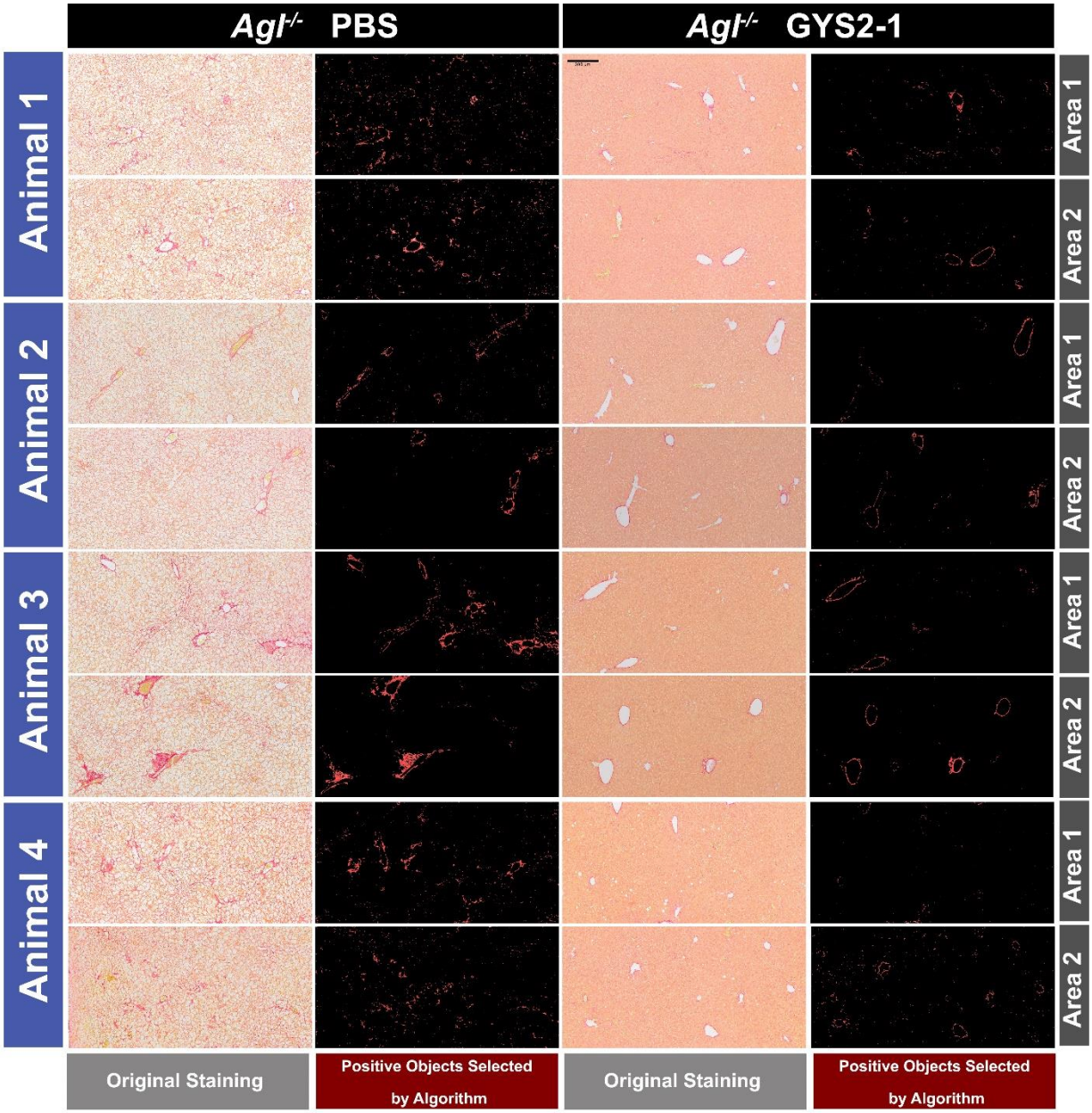

Quantitative analysis of Sirius Red staining in the liver of *Agl*$^{-/-}$ mice treated with PBS or GYS2-1 weekly for 18 doses starting at 8 weeks of age was performed using Olympus cellSens software. Briefly, two representative areas (approximately 2,000,000 μm² each) of one representative liver section for each individual animal were scored and quantified using an algorithm with a pre-defined intensity threshold. Certain areas were intentionally excluded from quantification in order to minimize the signal contributing from smooth muscles of large blood vessels. Examples of positive object selection using the algorithm are shown. The sum intensity normalized to the total area quantified was compared for PBS or GYS2-1 treated animals and the results summarized in Fig. 3C. Scale bar represents 200 μm.

Supplementary Fig. S7. GYS2-1 treatment prevents hepatomegaly in GSD III, *Agl*$^{-/-}$ mice.

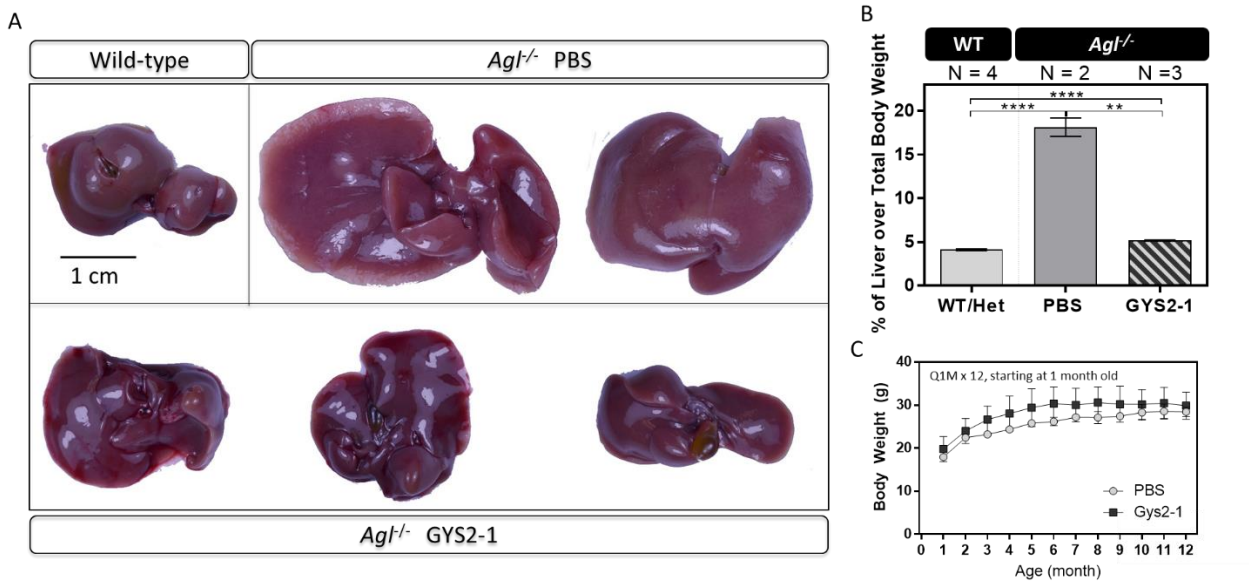

Agl$^{-/-}$ mice were treated with PBS or GYS2-1 monthly for 12 doses starting at 1 month of age. Liver samples were collected 72 hours following the final dose. (A and B) Inhibition of GYS2 synthesis with GYS2-1 treatment effectively prevents hepatomegaly in *Agl*$^{-/-}$ mice. Scale bar represents 1 cm. (** $p \leq 0.01$, **** $p < 0.0001$). (C) GYS2-1 treatment has no effects on growth rate of *Agl*$^{-/-}$ mice. Scale bar represents 1 cm.

Supplementary Fig. S8. Quantitative analysis of Sirius Red staining in PBS or GYS2-1 treated GSD III, *Agl*$^{-/-}$ mice in a long-term study.

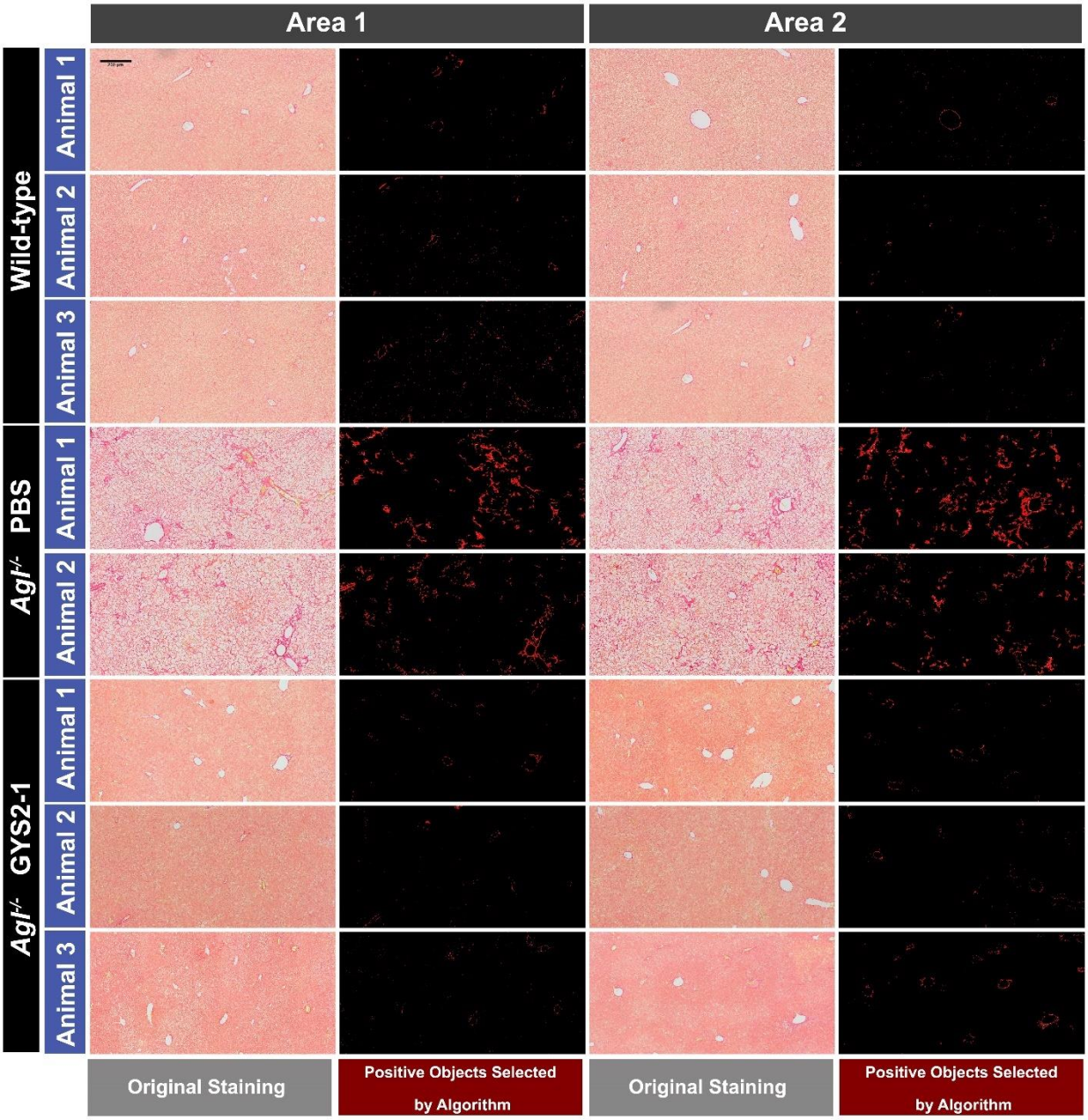

Quantitative analysis of Sirius Red staining in the liver of *Agl*$^{-/-}$ mice treated with PBS or GYS2-1 monthly for 12 doses starting at 1 month of age was performed using Olympus cellSens software. Briefly, two representative areas (approximately 2,000,000 μm² each) of one representative liver section for each individual animal were scored and quantified using an algorithm with a pre-defined intensity threshold. Certain areas were intentionally excluded from quantification in order to minimize the signal contributing from smooth muscles of large blood vessels. Examples of positive object selection using the algorithm are shown. The sum intensity normalized to the total area quantified

was compared for PBS or GYS2-1 treated animals and the results summarized in Fig. 6C. Scale bar represents 200 μm.

Supplementary Fig. S9. Histopathology analysis of growing nodule in *Agl*$^{-/-}$ mice.

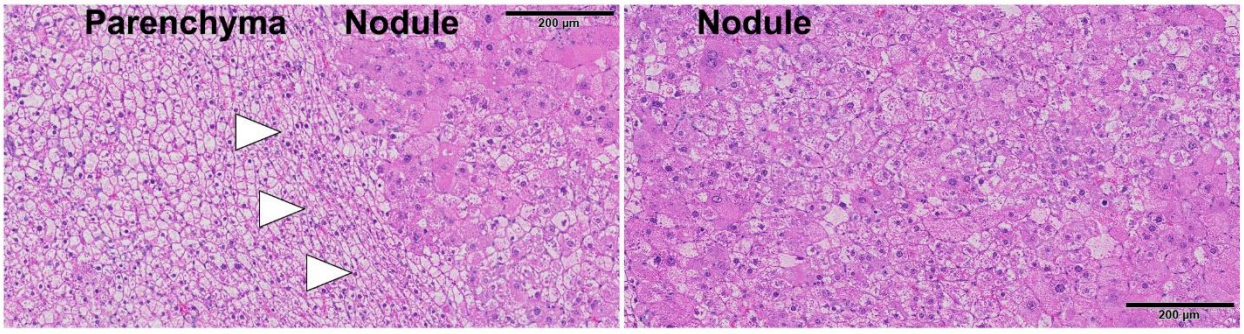

Agl$^{-/-}$ mice were treated with PBS or GYS2-1 monthly for 12 doses starting at 1 month of age. Liver samples were collected 72 hours following the final dose for H&E staining. Junction of parenchyma and nodule were indicated (arrowheads). Scale bar represents 200 μm.

Supplementary Fig. S10. No nuclear β-catenin staining was noted of growing nodules in *Agl*$^{-/-}$ mice.

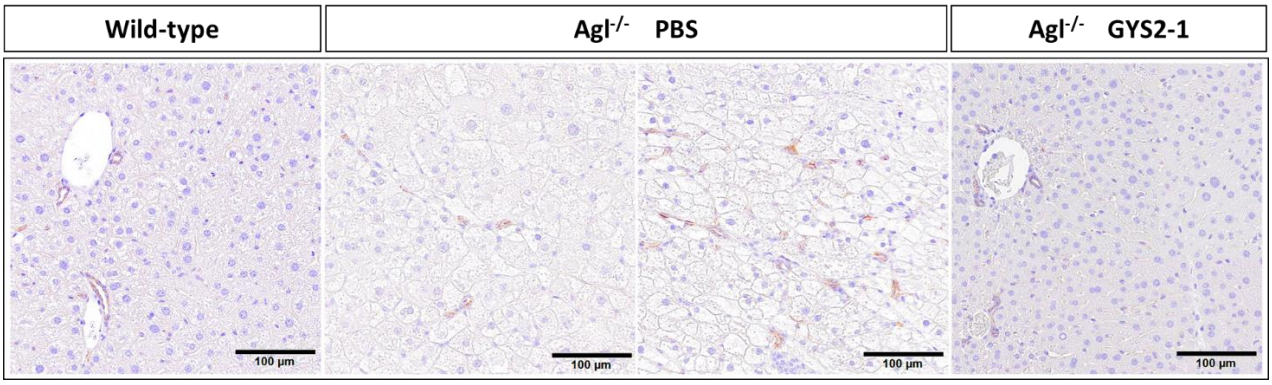

Agl$^{-/-}$ mice were treated with PBS or GYS2-1 monthly for 12 doses starting at 1 month of age. Liver samples were collected 72 hours following the final dose for β-catenin IHC. No nuclear β-catenin staining was noted in the nodules of PBS-treated *Agl*$^{-/-}$ mice. Scale bar represents 100 µm.

Supplementary Fig. S11. Correction of liver pathology thoroughly with GYS2-1 treatment in *Agl*$^{-/-}$ mice

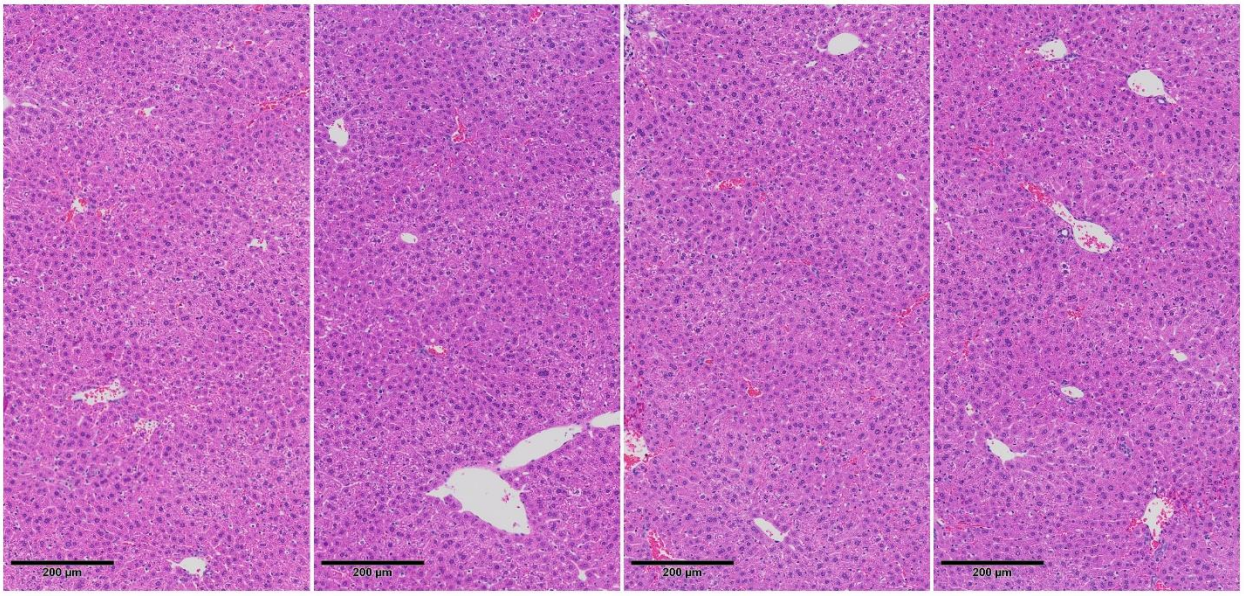

Agl$^{-/-}$ mice were treated with GYS2-1 monthly for 12 doses starting at 1 month of age. Liver samples were collected 72 hours following the final dose for histological analysis. H&E stained sections from four levels throughout the collected tissue sample are shown. The results demonstrate that GYS2-1 treatment fully reverses the liver pathology throughout the entire liver of *Agl*$^{-/-}$ mice until they are indistinguishable from their wildtype littermates. Scale bar represents 200 µm.

Supplementary Fig. S12. *L-G6pc*$^{-/-}$ mice have almost undetectable *G6pc* mRNA in the liver.

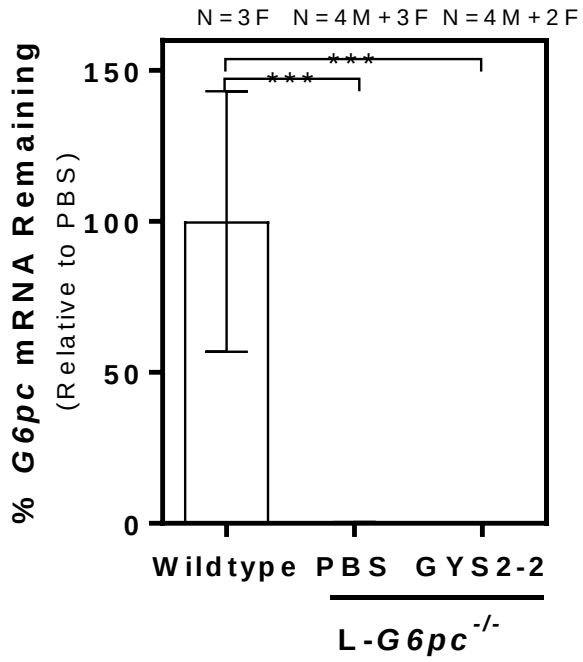

To generate *L-G6pc*$^{-/-}$ mice, G6Pase activity was disrupted specifically in the liver by temporal and tissue-specific deletion of the *G6pc* gene using CRE-lox strategy. In brief, conditional B6.G6pc$^{lox/lox}$ mice were crossed with transgenic B6.SA$^{creERT2/w}$ mice to generate B6.G6pc$^{lox/lox}$.SA$^{creERT2/w}$ mice, expressing inducible CREERT2 specifically in the liver. The treatment of adult B6.G6pc$^{lox/lox}$.SA$^{creERT2/w}$ mice with tamoxifen induced the excision of G6pc exon 3, specifically in the liver, leading to an undetectable hepatic *G6pc* mRNA detected by RT-PCR analysis of liver samples taken at the time of euthanasia after 5 doses of GYS2-2.

Supplementary Fig. S13. RNAi-mediated reduction of *Gys2* has no effect on glycemia, metaoblism, lipidemia, or body weight in mouse models of GSD Ia and GSD III.

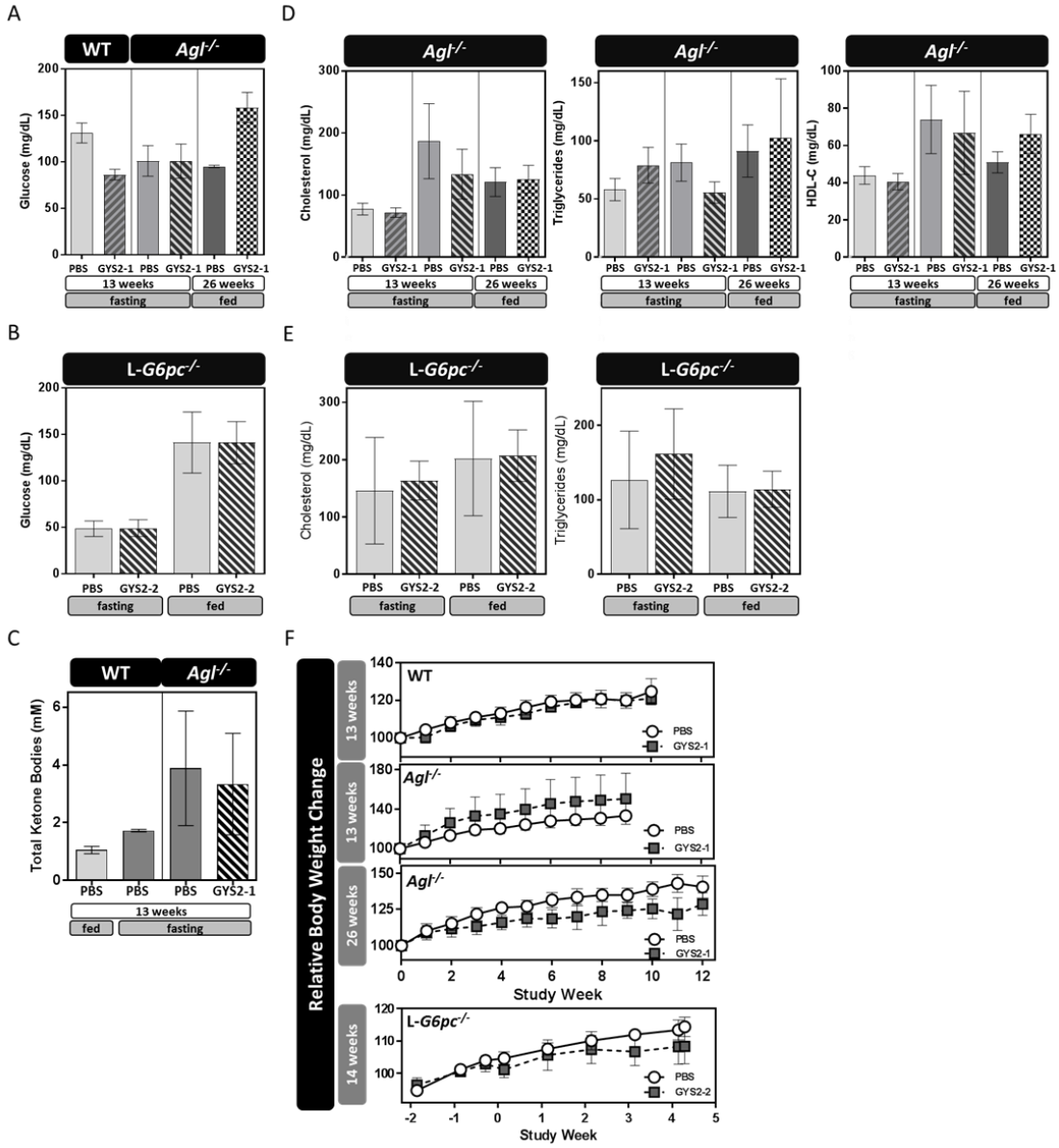

Liver-specific *Gys2* inhibition does not affect in glycemia in mouse models of (A) GSD III or (B) GSD Ia. (C) Increased levels of ketone bodies were measured in blood of *Agl*$^{-/-}$ mice during fasting indicating an increase in gluconeogenesis in the GSD III mouse model. GYS2-1 treatment had no effect on ketone body levels suggesting *Gys2* inhibition will not affect gluconeogenesis. Reduction of *Gys2* mRNA expression in the liver had no effects on lipidemia in GSD III (D) or GSD Ia (E) mice. (F) GYS2-1 and GYS2-2 treatment did not affect body weight of GSD III or GSD 1a mice, respectively.

Supplementary Fig. S14. GYS2-1 treatment does not reduce glycogen accumulation in skeletal muscle measured by PAS staining of formalin-fixed muscle tissue.

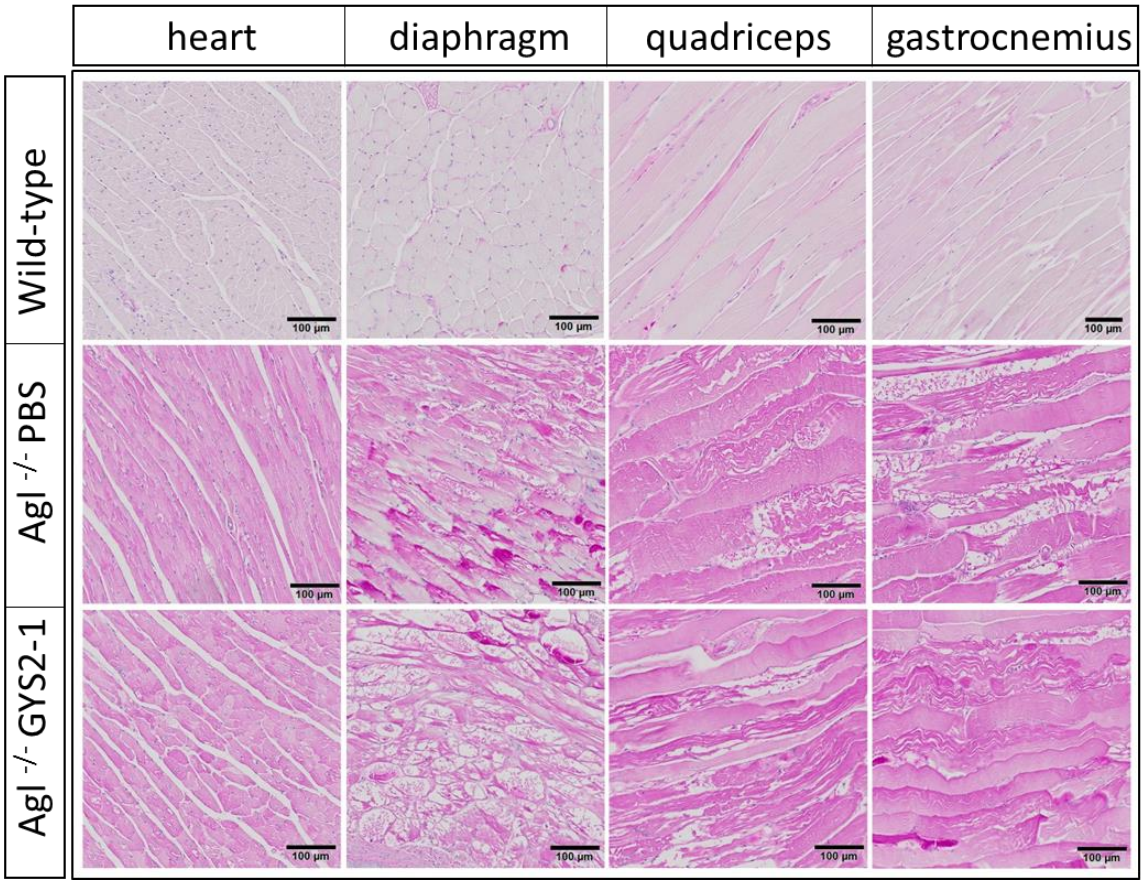

GalNAc-mediated delivery of siRNA conjugates mediated through the ASGPR receptor is liver-specific and GYS2-1 treatment has no effect on cardiac or skeletal muscle. Scale bar represents 100 µm.